

# Force Dynamics in Weakly Vibrated Granular Packings

Paul Umbanhowar<sup>1</sup> and Martin van Hecke<sup>2</sup>

<sup>1</sup>Department of Physics and Astronomy, Northwestern University, Evanston, IL 60208, USA.

<sup>2</sup>Kamerlingh Onnes Lab, Leiden University, PO box 9504, 2300 RA Leiden, The Netherlands.

(Dated: February 8, 2020)

A novel dynamical regime of granular matter is probed by weakly vibrating a grain filled column and measuring the variation of the force exerted on its bottom. While particle motions are minute, the bottom force exhibits a range of nonlinear and hysteretic behaviors that are indicative of strong and nontrivial force-network dynamics in weakly driven quasi-static granular media. For very weak vibrations a linear regime is attained where the bottom force modulations saturate with increasing mass in an oscillatory version of the Janssen effect.

PACS numbers: 45.70.-n, 05.45.-a, 43.25.Ts, 43.40.At

Granular media consist of macroscopic solid particles (grains) which interact via dissipative, repulsive contact forces and for which thermal energy is inconsequential. As a result, granulates *jam* in random configurations unless sufficient mechanical energy is supplied, for example by shearing or shaking [1]. In the case of sinusoidally and vertically vibrated granular media it is convenient to characterize the driving strength by the nondimensional peak acceleration,  $\Gamma = A(2\pi f)^2/g$ , where  $A$  is the displacement amplitude,  $f$  is the oscillation frequency, and  $g$  is the gravitational acceleration at the earth's surface. For  $\Gamma \gtrsim 1$ , grains loose contact with the container base and then subsequently collide: the resulting shock wave imparts kinetic energy to the grains which in turn allows the material to rearrange [2]. But when  $\Gamma < 1$ , the grains have been thought to simply comove with their vibrating container as a solid, jammed lump.

In this Letter we show that the system is far from static even in the  $\Gamma < 1$  driving regime: rather, it exhibits a rich set of dynamics in the *forces*. This finding does not contradict the absence of macroscopic grain motion, since for uncompressed granulates in the lab the length-scales setting the packing configuration (mm) and the gravity-induced contact forces ( $\mu\text{m}$ ) are effectively separated [3]. For example, a  $700\mu\text{m}$  diameter bronze sphere is compressed only  $\sim 100$  nm under the weight of 1000 additional identical spheres [4]. In addition, the contact forces in granulates are broadly distributed [1, 5] and organize into highly heterogeneous and fragile *force networks* [6, 7].

To probe the force dynamics in weakly vibrated granular media, we measure the variations of the total bottom force,  $F_b^{ac}$ , in a column filled with grains of total mass  $M$  [Fig. 1(a)]. Depending on  $\Gamma$ ,  $M$ , and  $f$ , we explore three different regimes: (i) For very weak driving,  $|F_b^{ac}|$  is linear in  $\Gamma$  but saturates for large  $M$ , qualitatively similar but quantitatively different from the static Janssen effect [8]. (ii) For strong driving, sliding of the grains is induced which leads to dramatic nonlinearities in  $F_b^{ac}$ . (iii) For most driving conditions, however, grain motion is minute, but  $F_b^{ac}$  evidences a strongly nonlinear and hysteretic re-

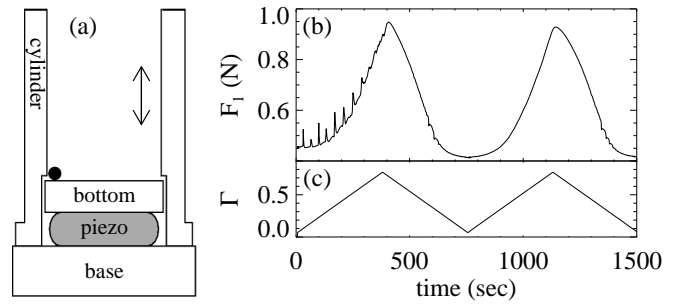


FIG. 1: (a) Sketch of the experiment, showing a piezo force sensor mounted between two aluminum cylinders, the “bottom” and the “base” (diameter  $\times$  height  $32 \times 12$  mm and  $89 \times 62$  mm respectively), with a cylindrical aluminum tube (inner/outer diameter  $30/55$  mm, height 113 mm), rigidly mounted to the base without making contact with the bottom. The gap between column and plate is  $\sim 100 \mu\text{m}$ , small enough to prevent grains (black dot) from becoming trapped. The entire assembly is weakly vibrated, and the sensor signal is used to obtain  $F_b^{ac}$ , the AC component of force exerted on the bottom plate by the grains. (b-c) Nonlinear response of a column filled with 200 g of grains under sweeps of the vibration strength  $\Gamma$  for  $f = 80$  Hz;  $F_1$  denotes the properly calibrated ratio of the first harmonic of  $F_b^{ac}$  and  $\Gamma$  (Eq. 1).

sponse of the material. Figures 1(b,c) illustrate this for 200 grams of material undergoing triangular sweeps of  $\Gamma$ . The strong increase of the force signal  $F_1$  with  $\Gamma$ , even for low frequencies, illustrates the main nonlinearity, since  $F_1$  is essentially the *ratio* of force-signal and  $\Gamma$  [see Eq. (1)]. This ratio is a constant for a solid mass placed onto the force sensor; here it doubles at  $\Gamma \sim 0.5$ . During the first ramp, the material compacts, causing the spikes in  $F_1$ ; apart from this no further macroscopic grain motion was detected. The asymmetry of  $F_1(\Gamma)$  is one manifestation of hysteresis and memory effects in compacted samples that will be discussed in detail below.

*Experimental Setup.* — In our experiment, nearly-spherical bronze particles sieved between 0.61 and 0.70 mm are poured into a smooth tube of which the bottom consists of a (piezo) force sensor with stiffness of 2.5 GN/m, and the entire assembly is vertically oscillated

with a small sinusoidal displacement; an accelerometer attached to the top of the column measures the time-resolved acceleration  $\gamma(t)$  which for most driving conditions is harmonic equaling  $\Gamma \sin(2\pi ft)$ . Minute deflections of force sensors can completely alter force configurations of granulates [7], but in our experiment the maximal sensor deflection is less than 1 nm, ensuring that measured force variations are intrinsic to the material [9, 10]. Similarly, the measured force is very sensitive to temperature drift, necessitating that the entire assembly be placed in an enclosure maintained slightly above room temperature (temperature fluctuations  $\pm 10$  mK, relative humidity 5-10%); grains are also stored in this box prior to use to equilibrate their temperature. More details are in Ref. [11].

The measured force signal  $F_{total}^{ac}$  is the sum of two components: the force from the acceleration of the bottom plate and sensor  $\propto \Gamma M_0$ , and the force  $F_b^{ac}$  from the acceleration of the grains (which can have harmonics):

$$F_{total}^{ac} = \Gamma M_0 g \sin(2\pi ft) + \Gamma \sum_{n=1}^{\infty} F_n \sin(2n\pi ft - \phi_n). \quad (1)$$

This implicit definition of  $F_n$  isolates the trivial scaling with  $\Gamma$ . We measured  $F_{total}^{ac}$  for a range of  $f$  and  $\Gamma$ , both with and without solid test masses attached to the bottom plate. The higher harmonics  $F_2, F_3, \dots$  are negligible and  $F_1$  is linear in the test mass and independent of  $\Gamma$ ; this allows us to subtract the component proportional to  $M_0 g$  and to calibrate the remaining signal.

*Linear Response.* — In the first set of experiments, we drive the systems weakly ( $\Gamma = 0.05$ ). Here  $F_b^{ac}$  remains harmonic (< 1% distortion) and in-phase with the acceleration, so that the signal is well characterized by  $F_1$  (which varies < 1% for  $0 < \Gamma < 0.1$ ). By incrementally pouring grains from a height of approximately 10 cm above the grain surface we create loose packings of increasing mass  $M$ . Figure 2 illustrates that  $F_1$  grows proportionally to  $M$  for small masses, but then rapidly saturates to  $F_1^{sat} \simeq 0.435$  N. Even though  $F_1(M)$  is weakly frequency dependent, the difference between the 16 Hz and 80 Hz curves is small, indicating that for low frequencies a well-defined quasi-static regime is probed. Note that for all frequencies a small overshoot occurs for intermediate values of  $M \sim 100$  g.

To interpret this result, it is helpful to discuss both the steady (DC) and alternating (AC) components of the total frictional wall-force  $F_w$  and the force normal to the bottom  $F_b$ . In the stationary case ( $\Gamma = 0$ ), the weight of the grains is carried by the wall and the bottom:  $Mg = F_w^{dc} + F_b^{dc}$ . In principle, the weight can be divided in numerous ways among bottom and sidewalls, but it is known for deep columns that  $F_b^{dc}$  saturates at a value  $F_{sat}^{dc}$  [8, 9, 12]. This saturation is termed the Janssen effect, and

$$F_b^{dc}/F_{sat}^{dc} = 1 - \exp(-Mg/F_{sat}^{dc}). \quad (2)$$

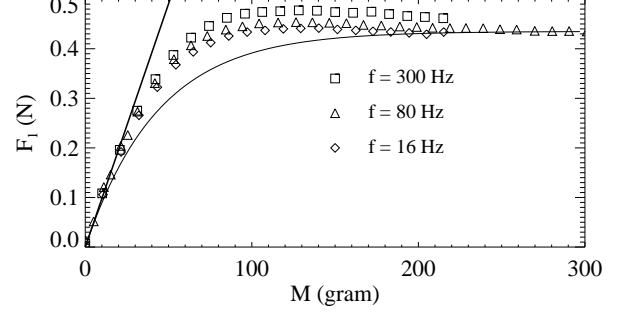


FIG. 2:  $F_1$  as function of the total grain mass  $M$  in the linear regime for  $f = 16, 80$  and  $300$  Hz, compared to a linear response (straight line) and a Janssen-like response  $F_1/F_{sat} = 1 - \exp(-Mg/F_{sat})$  for  $F_{sat} = 0.435$  N.

Our experiment can be seen as an oscillatory version of the Janssen experiment, since we accurately measure the *AC component* of the bottom force,  $F_b^{ac}$ , when the column is vibrated. If the packing does not slide with respect to the tube,

$$Mg\Gamma \cos(2\pi ft) = F_w^{ac} + F_b^{ac}. \quad (3)$$

Our measurements thus probe how the vibration induced *variations* of the grain weight,  $Mg\Gamma \cos(2\pi ft)$ , are distributed between wall and bottom.

How should  $F_1(M)$  be interpreted, and what is its relation to the DC Janssen effect? One might expect that  $F_1$  in a weakly *oscillating* column is proportional to the fraction of the total mass,  $M_{app} = F_b^{dc}/g$ , that rests on the bottom in a *stationary* column (this is equivalent to expecting that  $F_b^{dc}/F_w^{dc} = F_b^{ac}/F_w^{ac}$ ). However, as Fig. 2 shows, this is not the case.  $F_1$  significantly deviates from the static Janssen result (Eq. 2) when  $F_{sat}$  is equated with  $F_1(M=300\text{g})$ . We conclude that, even in the limit of weak vibrations, the force variations  $F_n$  are *not* simply related to the DC forces but instead probe variations of the force network that, for weak driving, may be described as an “elastic” response.

*Compaction.* — Before exploring the range of non-linear behaviors, we distinguish between “fresh” and “annealed” samples. “Spikes”, such as those shown in Fig. 1(b), occur when  $\Gamma$  is ramped up in “loose” samples, which can be created by placing a funnel on the bottom of the silo, filling it with material and then slowly retracting the funnel. Figure 3 illustrates that such spikes only occur in fresh territory, *i.e.* in samples for which  $\Gamma$  is increased beyond the previous maximum value of  $\Gamma$ . After  $\Gamma$  has been swept up once to a value close to 1, we refer to the sample as *fully annealed*. We interpret these spikes as due to wall-slippage and relative grain rearrangements. While initially stable packings of non-deformable grains should remain absolutely motionless under weak vibrations, real elastic grains deform under varying load. Since the frictional forces on the wall in carefully created granular columns are fully mobilized, *i.e.*, close to their maximal value, vibrations can cause

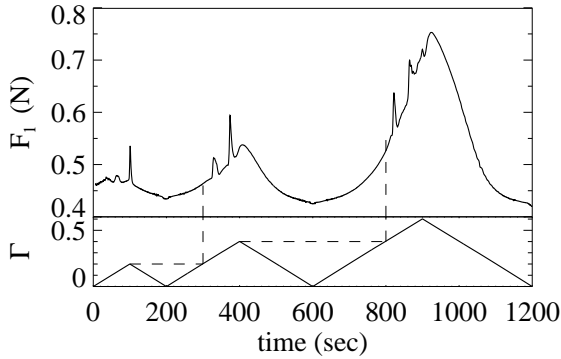


FIG. 3: Spikes observed for  $f = 80$  Hz and a loose packing of  $M = 200$  g. Sweeps of increasing magnitude in  $\Gamma$  illustrate that spikes only occur in “fresh” territory.

slippage, and stronger vibrations may cause further sliding. Consistent with this picture are the observations that the granulate is more compact after spikes occur and that gently poured columns produce more spikes than less gently prepared ones. Sliding is also consistent with the observations that, during the spikes (which last for 1000’s of vibration cycles), the phase shift  $\phi_1$  is significantly changed, the force signal is strongly non-sinusoidal, and the specific  $\Gamma$  values where spikes occur vary from run to run, and hence are not “resonant” effects.

*Nonlinear Response.* — By exploring the nonlinear response of fully annealed samples, we will show that the oscillatory transfer of forces between wall and bottom underlies the nonlinearity. We will distinguish a low frequency “contact” regime where this transfer is smooth, Eq. (3) is satisfied, and grains remain in contact with the bottom plate, and a high frequency “impact” regime where grains lose contact with the bottom plate and cause strong nonlinearities in both  $F_b^{ac}$  and  $\gamma(t)$ .

Starting with the contact regime, Fig. 4(a) illustrates that for small masses the grains are supported entirely by the bottom, since  $F_1 \approx Mg$ , while for larger  $M$ , wall forces start to play a role and  $F_1 < Mg$ ; this saturation goes hand in hand with an increasingly nonlinear response of the material with  $\Gamma$ . To check that no slipping occurs and Eq. (3) is satisfied, we have removed the cylinder from the setup, filled a separate but similarly sized, closed-bottom, cylindrical container with grains and placed it directly on the bottom plate. The sensor then becomes insensitive to smooth force transfers between the wall and the bottom of the container, and we find that in this case  $F_b^{ac}$  remains sinusoidal and  $F_1$  varies less than 1% when  $\Gamma$  is ramped between 0 and 0.9.

The nonlinearity in  $F_1(\Gamma)$  is accompanied by an increase in the harmonic distortion [13] of  $F_b^{ac}$  and an increase of the phase shift  $\phi_1$ . The waveform of the force signal for a strongly nonlinear case ( $\Gamma = 0.7$  and  $M = 200$  g) is shown in Fig. 4(b).  $F_1$  is doubled from its low  $\Gamma$  value for these driving parameters, while the harmonic distortion is only 6% and  $\phi_1 \approx 6^\circ$ . To understand this

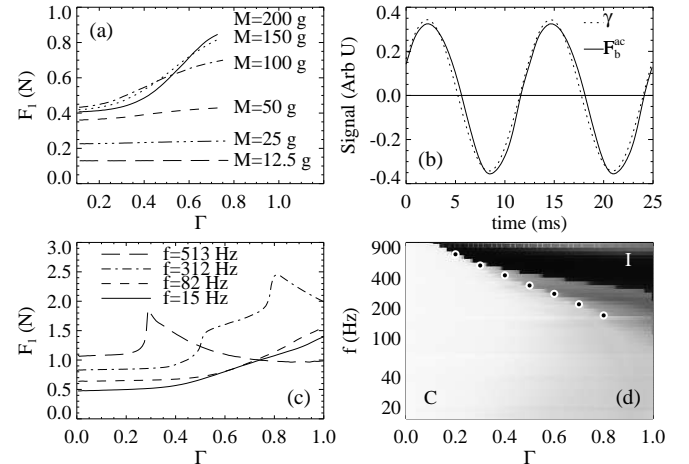


FIG. 4: Nonlinear response of force signal. (a)  $F_1(\Gamma)$  for various filling fractions ( $f = 80$  Hz). (b)  $\gamma(t)$  and  $F_b^{ac}$  for  $\Gamma = 0.7$  and  $M = 200$  g. The acceleration  $\gamma(t)$  is nearly perfectly sinusoidal, but the force signal lags behind and is non-harmonic. (c)  $F_1(\Gamma, f)$  for  $M = 200$  g shows smooth curves for low frequencies, but sudden upturns and peaks for higher frequencies (curves vertically offset for clarity). (d) Greyscale plot of nonlinearity  $\mathcal{N}(\Gamma, f) := F_1(\Gamma, f) - F_1(0, f)$  (white:  $\mathcal{N} = 0$ , black:  $\mathcal{N}$  positive) for  $M = 200$  g indicating the contact ( $C$ ) and impact ( $I$ ) regimes. The dots mark where the initial upturn in  $F_1$  occurs.

distortion, we note that when  $F_b$  and  $F_w$  vary strongly, so too does the pressure near the bottom. Due to the nonlinear Hertzian contact law [4], grains are stiffer when compressed, leading to an asymmetry between positive and negative variations of the effective gravity. Consistent with this picture, the peak in  $F_b^{ac}$  is suppressed while the minimum is enhanced [Fig. 4(b)].

Figure 4(c) illustrates that for low frequencies  $F_1$  increases smoothly with  $\Gamma$ , while for higher frequencies there is a sudden upturn and peak in the nonlinearity. In the vicinity of and above this change in behavior,  $\gamma(t)$  and  $F_b^{ac}$  become strongly anharmonic — similar to when grains loose contact with and periodically *impact* on the bottom for  $\Gamma > 1$  at low frequencies. Below this peak  $\gamma(t)$  remains perfectly sinusoidal. In the closed-bottom container (mentioned above), we observe similar nonlinearities in  $F_b^{ac}$  and  $\gamma(t)$  and thus a breakdown of Eq. (3).

To map out the contact and impact regimes, Fig. 4(d) presents the strength in the nonlinearity of  $F_1$  as function of  $\Gamma$  and  $f$ . We distinguish two regimes. In the contact region  $C$ ,  $\gamma(t)$  is sinusoidal, grains do not slip and  $F_1$  for the closed column is independent of  $\Gamma$ . In region  $I$ , in contrast, slippage and impact occur, and for both the ordinary column and closed-bottom containers  $\gamma(t)$  is strongly anharmonic. The boundary between  $C$  and  $I$  varies with  $M$  but not with the total mass of the cylinder, so a trivial resonance of the apparatus can be excluded [11]. Note that at high frequency ( $f \gtrsim 1$  kHz), the impact regime occurs for very small  $\Gamma$  ( $\sim 0.1$ ), a surprising finding given that relative grain motion has been

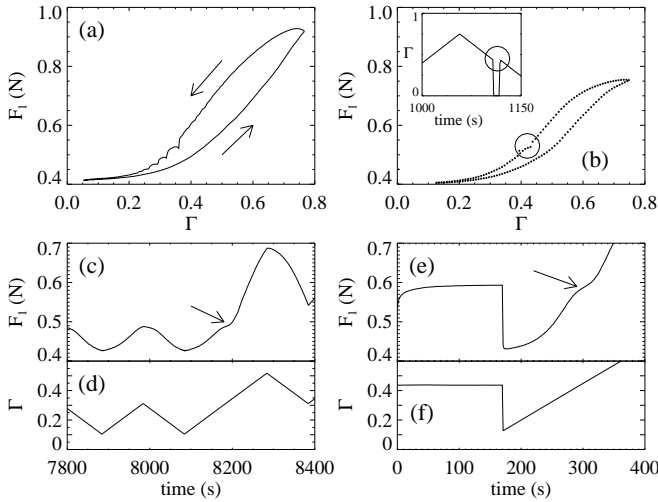


FIG. 5: Memory effects for  $M = 200$  g and  $f = 80$  Hz (a) Hysteresis loop. (b) Hysteresis persists when  $\Gamma$  is suddenly set to zero and then rapidly ramped back up, indicated by the circle (see inset for details of ramp). (c-f) Two examples of subtle memory effects.

thought to occur only for  $\Gamma > 1$ . This is likely related to the fact that for high frequencies standing waves can be excited in the material, leading to resonances; indeed we find that for smaller filling heights the impact regime occurs at higher frequencies [11].

*Hysteresis and Memory.* — So far, our data is consistent with a simple nonlinear response of the material, but Fig. 5(a) indicates that when  $\Gamma$  is ramped up and down in the nonlinear regime,  $F_b^{ac}$  is also hysteretic. The magnitude of hysteresis follows the same trend as the magnitude of nonlinearity, and, while the exact form of the hysteresis curve depends on the driving history, it is nearly independent of the sweep speed (for sweep durations longer than  $\approx 100/f$ ) and is only weakly dependent on the driving frequency. The force configuration thus depends on the driving history, and Fig. 5(b) illustrates that this configuration can be “frozen” since the system “remembers” it was on the upper branch of the hysteresis loop after the driving is switched off and then rapidly ramped up again. The system exhibits many more subtle memory effects: After a fully annealed system is subject to a number of small amplitude sweeps in  $\Gamma$ , and then  $\Gamma$  is ramped beyond the peak value of the small sweeps, a clear ‘kink’ in the  $F_1$  curve is exhibited [Fig. 5(c,d)]. When a fully annealed system is driven at a fixed value of  $\Gamma$ , it “remembers” this value when  $\Gamma$  is rapidly decreased then ramped past this value [Fig. 5(e,f)].

*Discussion.* — Our experiments provide evidence for a wide range of complex force dynamics in weakly vibrated granular media. In our system, the small shaking strength and low frequency allow us to explore the system in the quasi-static regime where the relative motion of grains is very small and the behavior of the material is dominated by variations in the force network, while the

extreme stiffness of our sensor (2.5 GN/m) ensures that the measured force variations are intrinsic to the material. This approach avoids complications due to relative motion between force probe and material that occurred in earlier work on weakly vibrated granulates [10].

How should we think about weakly vibrated granular systems? The contact laws between elastic bodies display a variety of nonlinear and hysteretic behaviors, allowing for rich behavior when many of these contacts are present [4, 14]. Our experiments present experimental evidence for this type of behavior, both in dynamic and in quasistatic regimes; for much higher driving frequencies, acoustic propagation experiments using a localized source observed possibly related complex behavior of grains [15]. We suggest that in our system the weak vibrations “activate” the force network, which then explores many different configurations consistent with the overall boundary conditions for the stress [3, 16]. In this sense, weakly vibrated granulates cannot be thought of as an ordinary solid.

The authors thank CATS and NWO who supported numerous visits to NWU during which this work was carried out.

---

- [1] A. J. Liu and S. R. Nagel, *Nature* **396**, 21 (1998); C. S. O’Hern, S. A. Langer, A. J. Liu, and S. R. Nagel, *Phys. Rev. Lett.* **88**, 075507 (2002).
- [2] J. Bougie, S. J. Moon, J. B. Swift, and H. L. Swinney, *Phys. Rev. E* **66**, 051301 (2002).
- [3] J. H. Snoeijer, T.J.H. Vlugt, M. van Hecke and W. van Saarloos, *Phys. Rev. Lett.* **92**, 054302 (2004).
- [4] K. L. Johnson, *Contact Mechanics*, Cambridge University Press (1987).
- [5] C. S. O’Hern, S.A. Langer, A. J. Liu and S. R. Nagel, *Phys. Rev. Lett.* **86**, 111 (2001).
- [6] D. W. Howell, R.P. Behringer and C.T. Veje, *Chaos* **9**, 559 (1999).
- [7] L. Vanel, D. Howell, D. Clark, R.P. Behringer and E. Clément, *Phys. Rev. E* **60**, R5040 (1999).
- [8] H. A. Janssen, Z. Ver. Dtsch. Ing. **39**, 1045 (1895).
- [9] G. Ovarlez, C. Fond and E. Clément, *Phys. Rev. E* **67**, 060302(R) (2003).
- [10] G. D’Anna and G. Gremaud, *Nature* **413**, 407 (2001); G. D’Anna, P. Mayor, G. Gremaud, A. Barrat and V. Loreto, *Europhys. Lett.* **61**, 60 (2003).
- [11] P. Umbanhowar and M. van Hecke, in preparation.
- [12] P. G. de Gennes, *Rev. Mod. Phys.* **71** 374-382 (1999).
- [13] The harmonic distortion of  $F_b^{ac}$  is defined as  $\sqrt{\sum_{i=2}^{\infty} F_i^2} / F_1$ .
- [14] F. Alonso-Marroquin and H.J. Herrmann, *Phys. Rev. Lett.* **92**, 054301 (2004).
- [15] C. H. Liu and S. R. Nagel, *Phys. Rev. Lett.* **68**, 2301, 1992.
- [16] J.P. Bouchaud, Proceedings of the 2002 Les Houches Summer School on *Slow Relaxations and Nonequilibrium Dynamics in Condensed Matter*.